Korean J. Chem. Eng., **21**(3), 680-688 (2004)

Numerical and Experimental Study on the Biofiltration of Toluene Vapor

Ho-Suk Choi† and Sung-Woon Myung

Department of Chemical Engineering, Chungnam National University, Daejeon 305-764, Korea
(*Received 16 April 2003 • accepted 18 December 2003*)

Abstract−We have solved both steady state and transient problems on the biofiltration of toluene vapor. The effect of inlet toluene concentration and inlet gas-flow rate on the removal rate of toluene and the elimination capacity of a lab-scale biofilter has been investigated. In this study, the effectiveness factor was a function of pollutant concentration. The dynamic solutions show good agreement with experimental results. At an inlet toluene concentration of 100 ppm, the diffusion of toluene into biofilm was obviously a rate determining step. Above 200 ppm, however, biofilm already showed full activity. The steady-state simulation confirmed that the change of elimination capacity obtained by increasing only inlet toluene concentration was the same as that obtained by increasing only flow rate of contaminated air. The maximum possible performance is about 20 g/m^3h with no addition of nutrients.

Key words: Biofiltration, Toluene, Modeling, Simulation, Elimination Capacity, Removal Efficiency

INTRODUCTION

Biofiltration is an APC (air pollution control) technology in which microorganisms are immobilized on organic/inorganic packing materials at an off-gas containing biodegradable volatile organic or inorganic compounds and is often a high-efficiency and low-cost alternative to other, more conventional, air pollution control technologies such as thermal oxidation, catalytic incineration, refrigerated condensation, carbon adsorption by chemicals and water scrubbers [Devinny and Deshusses, 1999]. The principle of biofiltration consists of a biologically active bed through which the contaminated off-gas is vented. Filter bed contains peat, compost, bark, soil or these mixtures with organic or inorganic inert materials that serve as carriers for microorganisms, nutrients and water. Aerobic biodegradation of organic pollutants occurs with the formation of CO_2, H_2O and biomass [Oh et al., 2002].

Biofiltration is a very complex hybrid technology that involves adsorption, absorption and biochemical reaction. Up to now, numerous efforts have been made to model the process [Chaudhary et al., 2003; Lim and Lee, 2003]. In the late 1970s, Jennings et al. [1976] and Ottengraf [1977] first suggested biofilm models with assumptions of basic mass balance principles, simple kinetics, and a plug flow air stream. These models answered the value of overall order of reaction occurring in biofilms. Shareefdeen et al. [1993, 1994a, b] proposed both steady-state and transient models in which the biodegradation was assumed to be first order with respect to both oxygen and the organic pollutant. The idea of their study was that some pollutants were adsorbed on the bare surface of support media while others were absorbed on the biofilm partially covering on the support media. Hodge and Devinny [1995] used an axially dispersed plug-flow model for gas phase and a linear driving force (LDF) model to approximate the interface mass transfer kinetics. They regarded the biofilm and the support media as a unified phase represented by a single, average concentration and assumed the pollutant degradation to be first order with respect to its average concentration in the unified phase. Deshusses et al. [1995] proposed a transient model for biofiltration of methyl ethyl ketone/methyl isobutyl ketone mixtures in which kinetic interaction between the pollutants was taken into account in the degradation reaction model. Abumaizar et al. [1997] studied the removal of BTEX (benzene, toluene, ethyl benzene and xylene) and investigated the effect of adding GAC to the compost biofilter. Their model described the basic transport of VOCs from the gas phase into the liquid phase by Fick's law. For the kinetics of biological degradation of substrate, they used a Monod-like relationship. Recently, Amanullah et al. [1999] developed a rigorous biofilter model to examine the effects of various operating variables and intrinsic properties on the transient response and conversion achieved at steady state. Their model incorporated convection and dispersion in the gas phase, partial coverage of the solid support, interphase mass transfer between the gas and the aqueous biofilm with an equilibrium partition at the interface followed by diffusion, direct adsorption to the exposed uncovered solid adsorbent media, transfer between the biofilm and the solid support, and biological reactions in both the biofilm and the adsorbent.

The main objective of this study is to make the numerical program of a rigorous model which enables us to study the effect of each parameter. Since both simulation and experiment allow us to fully understand the process, we tried to make both tools to well understand the biofiltration. In this study, we first solved a steady state problem of the biofilter process based upon Shareefdeen et al.'s model [1994b]. To match steady-state simulation results with experimental results, we adjusted the kinetic constants of the biodegradation reaction and determined some unknown parameters including specific surface area of the support media and biofilm thickness. The effect of inlet load on the removal efficiency or the elimination capacity has been investigated. We also solved the dynamic problem of a biofilter model suggested by Amanullah et al. [1999]. Through the simulation, we also examined the performance of a biofilter under given conditions and the relationship between operating parameters such as the inlet concentration of toluene and the flow rate of contaminated air.

†To whom correspondence should be addressed.
E-mail: hchoi@cnu.ac.kr

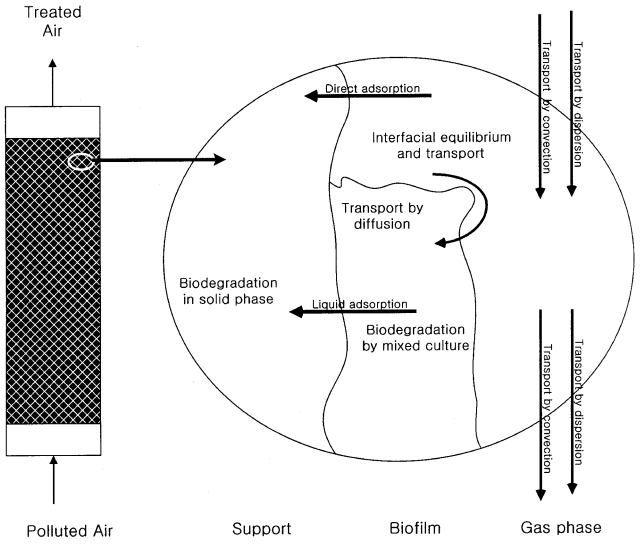

Fig. 1. Model concept of the biofiltration in a lab-scale biofilter.

MODEL DEVELOPMENT AND ANALYSIS

The model considers diffusion, convection, absorption, and biodecomposition of pollutants in the air stream occurring during biofiltration. The basic concepts of the model are explained schematically in Fig. 1. The assumptions of the model are as follows:

(i) The process is isothermal and the gas phase is assumed to be an ideal gas.
(ii) The radial dispersion of air stream is neglected through the packed bed and only the axial dispersion is considered.
(iii) The frictional pressure drop is neglected.
(iv) Pollutants and air in gas phase are always in equilibrium with those in liquid phase by following the Henry's law.
(v) Pollutants are aerobically decomposed in both the biofilm and the adsorbent.
(vi) Pollutants and oxygen are fully supplied by only diffusion through the biofilm.
(vii) The density of microbes and the thickness of biofilm are constant in the biofilter.
(viii) Since the thickness of the biolayer is much smaller than the size of filter media, pollutants and oxygen are transported only in one direction which is perpendicular to the surface of biofilm.
(ix) Diffusivities of the components in the biofilm are those in water corrected by a factor given by the correlation of Fan et al. [1990].
(x) The filter media is partially covered with the biofilm and the remaining bare surface is directly contacted with pollutants and air.
(xi) Pollutants are only adsorbed onto the bare surface of filter media.
(xii) The adsorption of pollutants is assumed to be linear, since the pollutant concentration is usually very low.
(xiii) The mass transfer of pollutants into the filter media is approximated by an LDF (linear driving force) model.

With the above assumptions, the governing equations are as follows.

1. Mass Balance in the Biofilm

In the biofilm, pollutants and oxygen are transported by diffusion and consumed by microbes.

Component balances are

$$\frac{\partial s_i}{\partial t} = D_i \frac{\partial^2 s_i}{\partial x^2} - R_{i,film} \tag{1}$$

and

$$\frac{\partial s_o}{\partial t} = D_o \frac{\partial^2 s_o}{\partial x^2} - R_{o,film} \tag{2}$$

where the initial conditions are

$$s_i(z, x, 0)=0 \tag{3}$$

$$s_o(z, x, 0)=0 \tag{4}$$

and the boundary conditions are

$$s_i(z, 0, t)=c_i/m_{1,i} \tag{5}$$

$$-\alpha A_s D_i \frac{\partial s_i(z,\delta,t)}{\partial x} = k_{i,l\text{-}ads}(q^*_{i,g\text{-}ads} - q_i) \tag{6}$$

$$s_o(z, 0, t)=c_o/m_o \tag{7}$$

$$\frac{\partial s_o(z,\delta,t)}{\partial x} = 0 \tag{8}$$

2. Mass Balance in the Gas Phase

While air streams including pollutants are transported by convection and diffusion through the biofilter, some pollutants and oxygen are transported into both the biofilm and the pore of filter media. Component balances are

$$\frac{\partial c_i}{\partial t} = D_l \frac{\partial^2 c_i}{\partial z^2} - \upsilon \frac{\partial c_i}{\partial z} - \frac{1-\varepsilon}{\varepsilon} \times \left[-\alpha A_s^* D_i \frac{\partial s_i}{\partial x}\bigg|_{x=0} + (1-\alpha) k_{i,g\text{-}ads}(q^*_{i,g\text{-}ads} - q_i) \right] \tag{9}$$

$$\frac{\partial c_o}{\partial t} = D_i \frac{\partial^2 c_o}{\partial z^2} - \upsilon \frac{\partial c_o}{\partial z} + \frac{1-\varepsilon}{\varepsilon} \alpha A_s D_o \frac{\partial s_o}{\partial x}\bigg|_{x=0} \tag{10}$$

where the initial conditions are

$$c_i(z, 0)=0 \tag{11}$$

$$c_o(z, 0)=0 \tag{12}$$

and the boundary conditions are

$$c_i(0, t)=c_{i,0} \tag{13}$$

$$\frac{\partial c_i(L,t)}{\partial z} = 0 \tag{14}$$

$$c_o(0, t)=c_{o,0} \tag{15}$$

$$\frac{\partial c_o(L,t)}{\partial z} = 0 \tag{16}$$

3. Mass Balance on the Surface of Filter Media

Pollutants are adsorbed on both the liquid layer and solid surface.

The balance equation is

$$\frac{\partial q_i}{\partial t} = \alpha k_{i,l\text{-}ads}(q^*_{i,g\text{-}ads} - q_i) + (1-\alpha) k_{i,g\text{-}ads}(q^*_{i,g\text{-}ads} - q_i) - R_{i,ads} \tag{17}$$

where the initial condition is

$$q_i(z, 0)=0 \tag{18}$$

Biodecomposition reaction in the biofilm:

Biodecomposition of pollutants in the biofilm can be expressed by the following

Baider interactive model [1982]:

$$R_{i,film}(s_i, s_o) = R_{max,i}\frac{s_i}{k_{m,i}\left(1+\frac{s_i^2}{k_{I,i}k_{m,i}}\right)+s_i}\frac{s_o}{k_{o,i}+s_o} \tag{19}$$

$$R_{o,film}(s_i, s_o) = R_{max,o}\frac{s_i}{k_{m,i}\left(1+\frac{s_i^2}{k_{I,i}k_{m,i}}\right)+s_i}\frac{s_o}{k_{o,i}+s_o} \tag{20}$$

Biodecomposition of pollutants in the adsorbent is assumed to be an *n*th-order reaction

$$R_{i,ads}=k_{rxn,i}q_i^{n'} \tag{21}$$

4. Adsorption Isotherm

Pollutants are adsorbed on the surface of filter media and the adsorption isotherm of pollutants is assumed to be the Freundlich equation:

$$q_{i,g\text{-}ads}^{*}=c_i/m_{2,i} \tag{22}$$

5. Numerical Analysis

The above set of partial differential equations is rewritten in dimensionless form as shown in Appendix I. Then, they are discretized in space (both in x and y direction), by using the method of orthogonal collocation, and become a set of ordinary differential equations. The discretizing procedure is explained in Appendix II. Nine inner points are used along the the biofilm thickness. Thus, the resulting ordinary differential equations become 189 coupled differential equations. The initial value problem is then integrated in the time domain by using Gear's BDF method provided in IMSL. Computation was continued until steady state was reached.

6. Steady-state Simulation

At steady state, the dimensionless governing equation can be rewritten as follows:

Mass balance in the biofilm:

$$\frac{\partial^2 Y_i}{\partial \xi^2}=\frac{\beta_5}{\beta_4}\frac{Y_i}{1+\beta_6 Y_i+\beta_7 Y_i^2}\frac{Y_o}{\beta_8+Y_o} \tag{23}$$

$$\frac{\partial^2 Y_o}{\partial \xi^2}=\frac{\beta_{10}}{\beta_9}\frac{Y_i}{1+\beta_6 Y_i+\beta_7 Y_i^2}\frac{Y_o}{\beta_8+Y_o} \tag{24}$$

with boundary conditions,

$$Y_i(\eta, 0)=X_i \tag{25}$$

$$Y_o(\eta, 0)=X_o \tag{26}$$

$$\frac{\partial Y_i(\eta, 1)}{\partial \xi}=0 \tag{27}$$

$$\frac{\partial Y_o(\eta, 1)}{\partial \xi}=0 \tag{28}$$

Mass balance in the gas phase:

$$\frac{\partial X_i}{\partial \eta}=\beta_1\left.\frac{\partial Y_i}{\partial \xi}\right|_{\xi=0} \tag{29}$$

$$\frac{\partial X_o}{\partial \eta}=\beta_3\left.\frac{\partial Y_o}{\partial \xi}\right|_{\xi=0} \tag{30}$$

with boundary conditions

$$X_i(0)=1 \tag{31}$$

$$X_o(0)=1 \tag{32}$$

The above partial differential equations are coupled with each other through boundary conditions. Thus, we first solved Eq. (23) and (24) at the initial section of biofilter bed and then solved Eq. (29) and (30) by using the first derivatives at the biofilm phase.

After determining the concentration of gas phase at the next section of biofilter bed, we again solved Eq. (23) and (24). With this procedure, we can sequentially solve the coupled differential equation from the inlet to the outlet.

To effectively solve the above equations, we combined Eq. (23) and (24) into one following equation.

$$\frac{\partial^2 Y_o}{\partial \xi^2}=\gamma_s\frac{\partial^2 Y_i}{\partial \xi^2} \tag{33}$$

with the boundary conditions, Eq. (25) to Eq. (28), where $\gamma_s=\beta_{10}\beta_4/\beta_9\beta_5$

The solution of Eq. (33) is

$$Y_o=\gamma_s(Y_i-X_i)+X_o \tag{34}$$

By substituting Eq. (34) into Eq. (23) and (29), we reduced the number of equations which have to be solved from four to two. We used the BVPFD and the DIVPRK in the IMSL library to solve Eq. (23) and (29), respectively.

7. Approximate Analysis

To investigate the effect of reaction kinetics on the removal of pollutants, we assumed two reaction kinetics: zero order and first order, respectively. Since the effect of oxygen concentration on the kinetics is not significant at the excess oxygen condition, we only take into account the effect of pollutant concentration on the kinetics. So, we assumed

$$\frac{Y_o}{\beta_8+Y_o}\approx 1 \tag{35}$$

When β_6 is much larger than other terms in the denominator of the right hand side of Eq. (23), Eq. (23) can be approximately written as the following zero-order kinetics:

$$\frac{\partial^2 Y_i}{\partial \xi^2}\approx \gamma_o \tag{36}$$

where

$$\gamma=\frac{\beta_5}{\beta_4\beta_6}.$$

After integrating Eq. (36) and applying boundary conditions, Eq. (25) and (27), we obtain

$$Y_i=\gamma_s\xi\left(\frac{\xi}{2}-1\right)+X_i \tag{37}$$

The first derivative of Eq. (37) at the interface between air and biofilm becomes

$$\left.\frac{\partial Y_i}{\partial \xi}\right|_{\xi=0} = -\gamma \tag{38}$$

Now, we can solve Eq. (29) in the gas phase. Thus, we have

$$X_i = 1 - \beta_1 \gamma \eta \tag{39}$$

where

$$\beta_1 = \left(\frac{1-\varepsilon}{\varepsilon}\right)\frac{\alpha A_s^* L \gamma_{max,i} \delta}{\upsilon c_{i,o}} \tag{40}$$

On the other hand, when β_6 and β_7 are much less than 1, the kinetics becomes first order.

$$\frac{\partial^2 Y_i}{\partial \xi^2} \approx \gamma_1 Y_i \tag{41}$$

where

$$\gamma_1 = \frac{\beta_5}{\beta_4}.$$

Applying the boundary conditions, Eqs. (25) and (27),

$$Y_i = \frac{\cosh\sqrt{\gamma_1}(1-\xi)}{\cosh\sqrt{\gamma_1}} X_i \tag{42}$$

The first derivative of Eq. (42) at ξ=0 is

$$\left.\frac{\partial Y_i}{\partial \xi}\right|_{\xi=0} = -\sqrt{\gamma_1}\tanh(\sqrt{\gamma_1} X_i) \tag{43}$$

Now, substituting Eq. (43) into Eq. (29), we have

$$X_i = e^{-\beta_1\sqrt{\gamma_1}\tanh(\sqrt{\gamma_1}\eta)} \tag{44}$$

where

$$\beta_1 = \left(\frac{1-\varepsilon}{\varepsilon}\right)\frac{L D_i \alpha A_s}{m_{1,i} \delta \upsilon}$$

and

$$\gamma_1 = \frac{\delta^2}{K_{mi}} \frac{\gamma_{max,i}}{D_i}.$$

EXPERIMENTAL

As represented in Fig. 2, we used the unit which was an acrylic column of 10.6 cm diameter and 160 cm height, equipped with a sampling port at each stage. The height of the biofilter bed was 120 cm, leading to a value of bed volume equal to 10.59×10^{-3} m^3. The packing material consisted of a mixture of peat and calstone (5 : 3 volume ratio before mixing). The microorganism used in the experiments was *Pseudomonas. Putida* type A and the strain of *Pseudomonas. Putida* is provided by Dr. Khoo, InBionet, Inc. The cells were maintained at 4 °C on agar plate. The culture medium used contained per liter: glucose, 1.1 g; NH_4Cl 0.1 g; $MgSO_4\cdot7H_2O$ 0.05 g; $FeSO_4\cdot7H_2O$ 0.005 g; $MnSO_4\cdot H_2O$ 0.005 g; $CaCl_2$ 0.00375 g; Yeast extract 1 g; 0.1 M phosphate buffer solution 18 ml. The microorganism cultured with the above medium in a shaking flask was well mixed with the packing materials and then packed into the column. The biofilter bed was supplied with a humidified air stream containing toluene vapor. We conducted the experiment under the conditions of the air flow rate of 10 L/min and the toluene concentrations of 100, 200, 300 ppm (which corresponds to 0.411, 0.821, 1.231 g/m^3, respectively). The air stream was divided into two streams. The main one was passed through a water vessel for humidification. The second stream was passed through a closed toluene vessel. And then two streams were mixed before they entered the biofilter bed. The flow rates of two streams were controlled by two flow meters, respectively. The concentration of toluene was measured by a portable GAS-TEC (Flame Ionization Monitor Type 47674, Telegan Gas Monitoring Ltd., West Sussex, England) detector. The temperature of the biofilter bed was kept from 25 °C to 30 °C for maintaining high microbial activity. To avoid the pressure drop in the biofilter bed due to compaction, whole column was divided by 4 stages. The pressure drop was measured at each stage by a manometer filled with water.

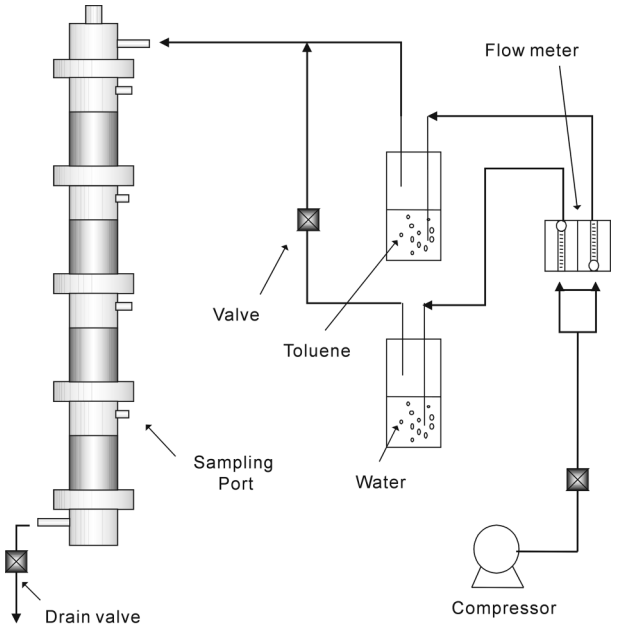

Fig. 2. Schematic diagram of experimental apparatus.

RESULTS AND DISCUSSION

Table 1 represents parameter values used for solving the model equations. We used IMSL library (DIVPRK for gas phase and BVPFD for biofilm) included in Digital Visual Fortran (Digital Equipment Corporation, Maynard, Massachusetts) to obtain numerical solutions of both steady-state and transient models. We first obtained the steady state solutions at the air flow rate of 10 L/min and the toluene concentrations of 100, 200, 300 ppm, respectively.

Fig. 3 represents both simulation and experimental results. Simulation results show good agreement with experimental results, especially at high toluene concentration. At low concentration of toluene, the experimental results fit very well with the first-order kinetic approximation while they fit very well with the zero-order kinetic

Table 1. Parameter values used for the simulation

Parameter	Value	Units
v	1.89	cm/s
L	120	cm
D_L	3.4×10^{-2}	cm^2/s
α	0.50	-
ε	0.30	-
$m_{1,i}$	0.27	-
$m_{2,i}$	0.02	-
m_0	34.40	-
As	1.78	1/cm
D_i	2.00×10^{-6}	cm^2/s
D_0	4.70×10^{-6}	cm^2/s
δ	3.76×10^{-4}	cm
$k_{ig\text{-}ads}$	3.20×10^{-4}	1/sec
$k_{il\text{-}ads}$	0	1/sec
$r_{max,i}$	14.99×10^{-5}	$g/cm^3/sec$
$r_{max,o}$	12.23×10^{-5}	$g/cm^3/sec$
$K_{m,i}$	1.00×10^{-6}	g/cm^3
$k_{m,o}$	0.26×10^{-6}	g/cm^3
$c_{i,0}$	$0.411\text{-}1.231\times10^{-6}$	g/cm^3
$c_{o,0i}$	2.75×10^{-4}	g/cm^3
$K_{I,i}$	0.05×10^{-6}	g/cm^3
$R_{rxn,i}$	0	-
N'	0	-

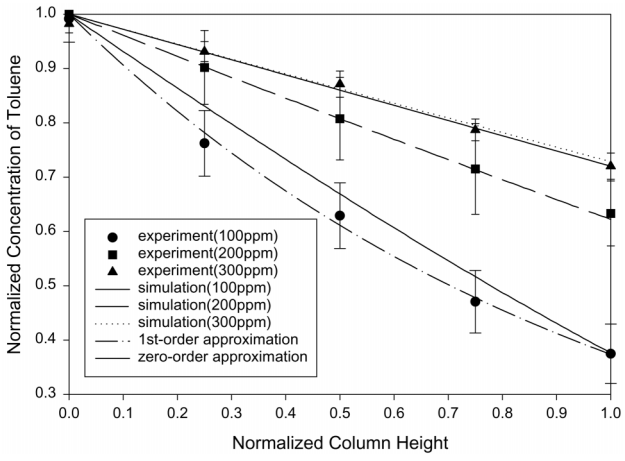

Fig. 3. Comparison of experimental data with steady state simulation results.

approximation at high concentration of toluene. Thus, the model parameter used in the Baider interactive model has to be carefully readjusted for low concentration kinetics. The simulation, however, predicts very well the exit toluene concentration of the biofilter.

We also plotted the elimination capacity as a function of inlet loads in Fig. 4. The elimination capacity is very important since it is related with the removal efficiency and inlet loads. The maximum elimination capacity is affected by the activity of microbes. The activity is a function of the environmental conditions such as temperature, humidity and inhibitory substances. Diks and Ottengraf [1991] reported various expressions of the elimination capacity, but the definition we used in this study is

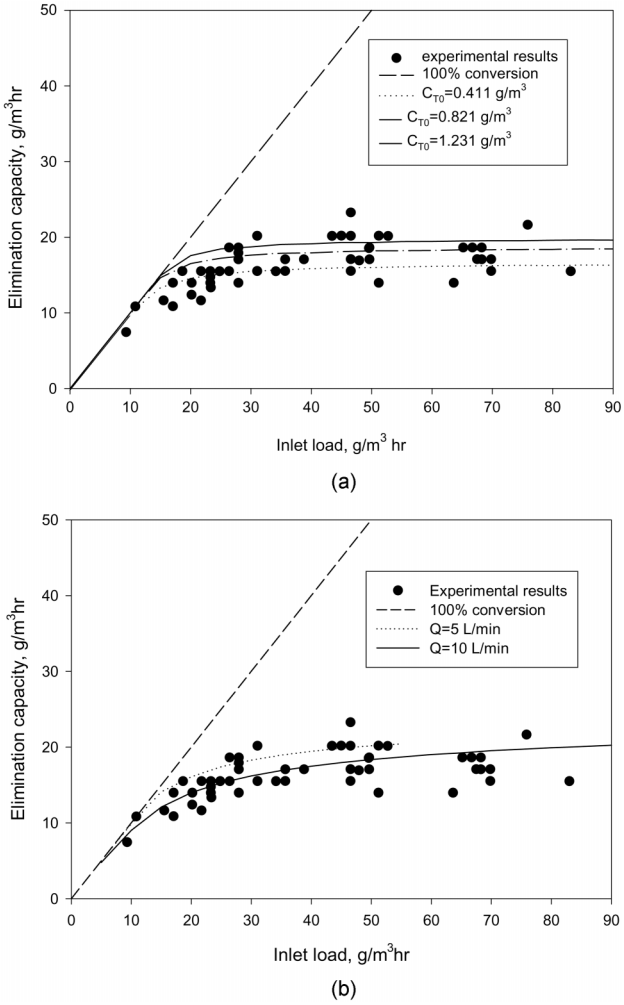

Fig. 4. Change of elimination capacity with respect to inlet load. (a) effect of inlet concentration of toluene, (b) effect of inlet flow rate

$$\text{E.C.} = \frac{(C_i - C_o)\times Q}{V_{bed}} \tag{45}$$

where V_{bed} is a volume of support media in biofilter and Q is a volumetric flow rate of air stream.

As shown in Fig. 4, the elimination capacity increases with increasing the contaminated airflow rate since the amount of toluene transported from air stream to biofilm increases with increasing inlet loads from 0 to 20 g/m^3hr. The elimination capacity, however, does not increase at the inlet loads of over 30 g/m^3hr. From this result, we can know that the activity of microbes in the biofilm reaches a maximum and the maximum elimination capacity of our system is about 20 g/m^3hr. Yoon et al. [2002] recently reported high value of elimination capacity after optimizing operating parameters such as temperature, residence time and inlet concentration in their compost-packed biofilter. It is thought to be that the low value of our maximum elimination capacity is due to the lack of nutrients during the operation. In Fig. 4(a), we also compared the experimental elimination capacities with simulation results obtained by changing the flow rate of air stream at constant inlet concentration of toluene.

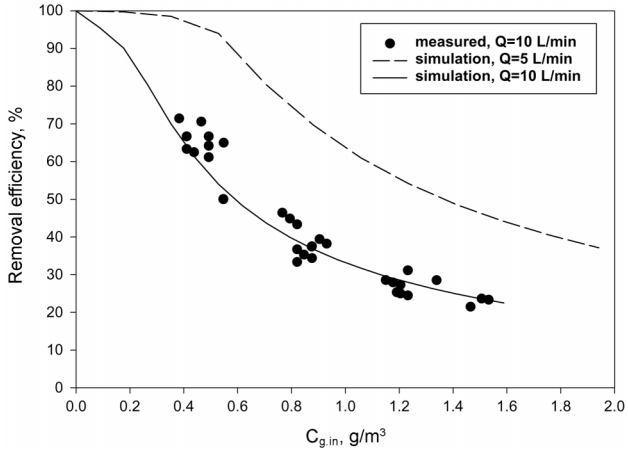

Fig. 5. Change of removal efficiency with respect to the inlet toluene concentration.

Simulation shows that the maximum elimination capacity depends on the inlet concentration of toluene. The maximum elimination capacity asymptotically approaches to a fixed value as the inlet concentration of toluene increases. In Fig. 4(b), we also investigated the effect of the flow rate on the elimination capacity by changing the inlet toluene concentration at constant flow rate. In this simulation, the elimination capacity increases with decreasing flow rate and asymptotically approaches a maximum value.

Fig. 5 represents the change of removal efficiencies with respect to the inlet concentration of toluene. The experiment was conducted at the toluene concentrations of 0.411 to 1.233 g/m^3 and the removal efficiency was obtained from dividing the difference between the inlet and the outlet toluene concentrations by the inlet toluene concentration. The removal efficiency of 65% at C_{T0}=0.411 g/m^3 decreases rapidly to about 35% at C_{T0}=0.821 g/m^3. At over C_{T0}=0.821 g/m^3, however, the removal efficiency decreases slowly. This is because, at low inlet concentration of toluene, the diffusion of toluene through biofilm is a rate determining step (as also observed at Fig. 3 with high curvature of 100 ppm line since, in case that we assumed zero order kinetics, the concentration profile became a second order function with respect to the height of column in the diffusion limited regime [Zarook, 1997].). The removal efficiency calculated at low flow rate (Q=5 L/min) is much larger than that calculated at Q= 10 L/min at the same inlet concentration of toluene.

We also calculated the effectiveness factor at three different inlet concentrations of toluene. The effectiveness factor is defined as follows:

$$e_T \text{ or } e_O = -D_i(ds_i/dx)_{x=0}/r_{max,\,i} \quad (46)$$

The effectiveness factor actually depends on the concentration of toluene as shown in the inset of Fig. 6 although its dependence is too small. At a toluene concentration above 0.8 g/m^3, the effectiveness factor becomes small and constant, which means that the diffusion is relatively slow as compared to the biodegradation rate and the diffusion may control the overall process. Although the effectiveness factor becomes large at low inlet concentration of toluene, the diffusion flux is still small as compared to the biodegradation rate. Thus, the whole process is mainly controlled by diffusion under fast-flow condition of this experimental system.

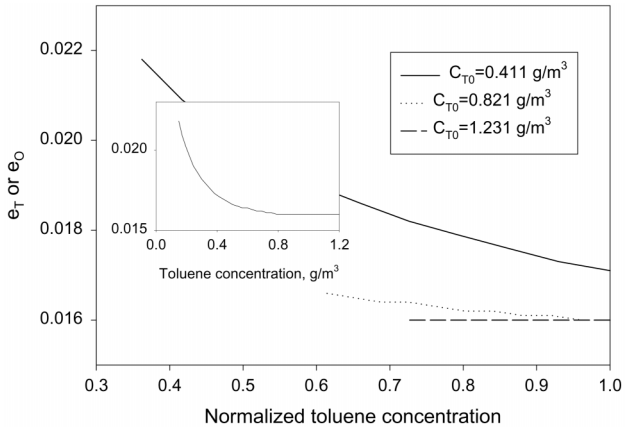

Fig. 6. Effect of inlet toluene concentration on the effectiveness factor.

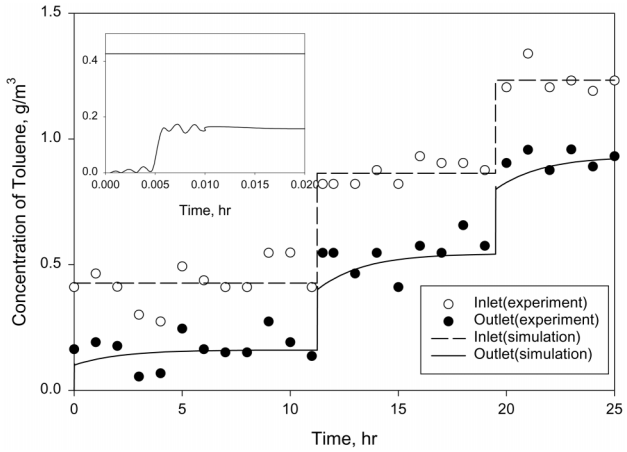

Fig. 7. Comparison of experimental data with the dynamic simulation results.

Fig. 7 shows the dynamic simulation results for the three step inputs. As shown in the inset of Fig. 7, the first response for the step input is at about 20 sec. The equilibrium, however, is reached at about 8 hours. This is because the process is a kind of reactive-adsorption, that is, the adsorbed toluene keeps being removed in the biofilm before it reaches equilibrium. The simulation results show good agreement with experimental results for the overall process. Under our experimental conditions, the space time is very small, that is, τ=19 sec. Thus, the untreated toluene is detected at about 20 sec after the initial step input. The exit toluene concentration, however, increases until it reaches the adsorption equilibrium. The same exit patterns are observed at the second and the third steps. But, at the second and the third steps, the filter media are already saturated under the condition of first step. Thus, the additional adsorption only proceeds until the toluene concentration reaches a new equilibrium for the step increase of inlet toluene concentration.

CONCLUSIONS

We successfully solved both steady state and transient problems of the biofilter process. Both simulation results show good agreement with experimental results. The removal efficiency decreased

with increasing the inlet concentration of toluene since biofilm activity eventually reached a limit as increasing the amount of dissolved toluene. Thus, the elimination capacity reached the maximum value of about 20 g/m^{3}hr at the inlet load of 30 g/m^{3}hr. At the inlet toluene concentration of 100 ppm, the diffusion of toluene into biofilm was obviously a rate determining step. Above 200 ppm, however, biofilm already showed full activity. The steady-state simulation confirmed that the change of elimination capacity obtained by increasing only inlet toluene concentration was the same as that obtained by increasing only flow rate of contaminated air. The fact allows us to extend the simulation to the prediction of the elimination capacity at other operating conditions without doing additional experiments. The effectiveness factor was a function of toluene concentration especially at low concentration of toluene. The overall process, however, was controlled by the diffusion of toluene through the biofilm phase. The dynamic solutions also show good agreement with experimental results obtained at three different step inputs. The initial response was very quick and not at equilibrium until the filter media were saturated by toluene under the given condition.

ACKNOWLEDGMENTS

This work was supported by the Korean Ministry of Science and Technology with the grant number of ENVIRONMENT-99-05.

APPENDIX I. DIMENSIONLESS FORM OF THE GOVERNING EQUATIONS

Mass balance in the gas-phase

$$\frac{\partial X_i}{\partial \tau}=\frac{1}{Pe}\frac{\partial^2 X_i}{\partial \eta^2}-\frac{\partial X_i}{\partial \eta}+\beta_1\frac{\partial Y_i}{\partial \xi}\bigg|_{\xi=0}+\beta_2(X_i-Z_i) \quad \text{(i)}$$

$$\frac{\partial X_o}{\partial \tau}=\frac{1}{Pe}\frac{\partial^2 X_o}{\partial \eta^2}-\frac{\partial X_o}{\partial \eta}+\beta_3\frac{\partial Y_o}{\partial \xi}\bigg|_{\xi=0} \quad \text{(ii)}$$

with initial conditions

$$X_i(\eta, 0)=0 \quad \text{(iii)}$$

$$X_o(\eta, 0)=0 \quad \text{(iv)}$$

and boundary conditions

$$X_i(0, \tau)=1 \quad \text{(v)}$$

$$X_o(0, \tau)=1 \quad \text{(vi)}$$

$$\frac{\partial X_i(1,\tau)}{\partial \eta}=0 \quad \text{(vii)}$$

$$\frac{\partial X_o(1,\tau)}{\partial \eta}=0 \quad \text{(viii)}$$

Mass balance in the biofilm:

$$\frac{\partial Y_i}{\partial \tau}=\beta_4\frac{\partial^2 Y_i}{\partial \xi^2}-\beta_5\frac{Y_i}{1+\beta_6 Y_i+\beta_7 Y_i^2}\frac{Y_o}{\beta_8+Y_o} \quad \text{(ix)}$$

$$\frac{\partial Y_o}{\partial \tau}=\beta_9\frac{\partial^2 Y_o}{\partial \xi^2}-\beta_{10}\frac{Y_i}{1+\beta_6 Y_i+\beta_7 Y_i^2}\frac{Y_o}{\beta_8+Y_o} \quad \text{(x)}$$

with initial conditions

$$Y_i(\eta, \xi, 0)=0 \quad \text{(xi)}$$

$$Y_o(\eta, \xi, 0)=0 \quad \text{(xii)}$$

and boundary conditions

$$Y_i(\eta, 0, \tau)=X_i \quad \text{(xiii)}$$

$$Y_o(\eta, 0, \tau)=X_o \quad \text{(xiv)}$$

$$\frac{\partial Y_i(\eta,1,\tau)}{\partial \eta}=-\beta_{11}(X_i-Z_i) \quad \text{(xv)}$$

$$\frac{\partial Y_o(\eta,1,\tau)}{\partial \eta}=0 \quad \text{(xvi)}$$

Mass balance on the surface of biofilter media:

$$\frac{\partial Z_i}{\partial \tau}=\beta_{12}(X_i-Z_i)-\beta_{13}Z_i^{n'} \quad \text{(xvii)}$$

with initial condition

$$Z_i(\eta, 0)=0 \quad \text{(xviii)}$$

where dimensionless groups are

$$Pe=\frac{L\upsilon}{D_l}\ \text{(Peclet number)},\quad \tau=\frac{\upsilon t}{L},\quad \xi=\frac{x}{\delta},\quad \eta=\frac{z}{L},\quad X_i=\frac{c_i}{c_{i,0}},$$

$$X_o=\frac{c_o}{c_{i,0}},\quad Y_i=\frac{m_{1,i}s_i}{c_{i,0}},\quad Y_o=\frac{m_o s_o}{c_{o,0}},\quad Z_i=\frac{m_{2,i}q_i}{c_{i,0}},$$

$$\beta_1=\left(\frac{1-\varepsilon}{\varepsilon}\right)\frac{\alpha}{m_{1,i}}\frac{A_s L D_i}{\delta\upsilon},\quad \beta_2=\frac{1-\varepsilon}{\varepsilon}\frac{1-\alpha}{m_{2,i}}\frac{k_{ig-ads}L}{\upsilon},\quad \beta_3=\frac{1-\varepsilon}{\varepsilon}\frac{\alpha}{m_0}\frac{A_s L D_o}{\delta\upsilon},\quad \beta_4=\frac{D_i L}{\delta^2\upsilon},$$

$$\beta_5=\frac{r_{max,i}L}{\upsilon k_{mi}},\quad \beta_6=\frac{c_{i,o}}{k_{mi}m_{1,i}},\quad \beta_7=\frac{c_{i,o}^2}{m_{1,i}^2 k_{I,i}k_{m,i}},\quad \beta_8=\frac{k_{o,i}m_o}{c_{o,0}},\quad \beta_9=\frac{D_o L}{\upsilon\delta^2},$$

$$\beta_{10}=\frac{r_{max\,o,i}L}{\upsilon k_{mi}},\quad \beta_{11}=\frac{m_{1,i}}{\alpha_{m2,i}}\frac{k_{i,l-ads}\delta}{A_s D_i},\quad \beta_{12}=(1-\alpha)\frac{k_{i,l-ads}L}{\upsilon}+\alpha\frac{k_{i,l-ads}L}{\upsilon},$$

$$\beta_{13}=\frac{k_{rxn,i}L}{\upsilon}\left(\frac{c_{go}}{m_2}\right)^{n'-1}.$$

APPENDIX II. DISCRETIZATION BY ORTHOGONAL COLLOCATION

To convert a set of partial differential equations into a set of ordinary differential equations, we used the orthogonal collocation method. First, we discretized the space into (n+2) roots of Jacobi polynomial between 0 and 1. Then, dependent variables (X_i, X_o, Y_i, Y_o, Z_i) were approximated as a linear combination of Lagrange polynomial.

For example,

$$X_i(\eta_i, \tau)=\sum_{j=1}^{n+2} l_j(\eta_i)X_{i,j}(\tau)\quad i=1, 2, 3\ldots, n+2 \quad \text{(i)}$$

where

$$l_j(\eta)=\prod_{k=1,k\neq j}^{n+2}\frac{\eta-\eta_k}{\eta_j-\eta_k} \quad \text{(ii)}$$

Let us denote $l_j(\eta_i)=L_{ij}$, $l_j(\xi_i)=L'_{ij}$

$$\frac{\partial l_j(\eta_i)}{\partial \eta}=A_{ij},\ \frac{\partial l_j(\xi_i)}{\partial \xi}=A'_{ij} \quad \text{(iii)}$$

$$\frac{\partial^2 l_j(\eta_i)}{\partial \eta^2} = B_{ij}, \frac{\partial^2 l_j(\xi_i)}{\partial \xi^2} = B'_{ij}$$

Then,

$$\frac{\partial X_j(\eta_i,\tau)}{\partial \eta} = \sum_{j=1}^{n+2} A_{ij} X_{i,j}(\tau), \frac{\partial^2 X_j(\eta_i,\tau)}{\partial \eta^2} = \sum_{j=1}^{n+2} B_{ij} X_{i,j}(\tau) \quad \text{(iv)}$$

$$\frac{\partial X_o(\eta_i,\tau)}{\partial \eta} = \sum_{j=1}^{n+2} A_{ij} X_{o,j}(\tau), \frac{\partial^2 X_o(\eta_i,\tau)}{\partial \eta^2} = \sum_{j=1}^{n+2} B_{ij} X_{o,j}(\tau) \quad \text{(v)}$$

$$\frac{\partial Y_i(\eta_i,\xi_k,\tau)}{\partial \xi} = \sum_{j=1}^{n+2} A'_{kj} Y_{i,j}(\eta_i,\tau), \frac{\partial^2 Y_i(\eta_i,\xi_k,\tau)}{\partial \xi^2} = \sum_{j=1}^{n+2} B'_{kj} Y_{i,j}(\eta_i,\tau) \quad \text{(vi)}$$

$$\frac{\partial Y_o(\eta_i,\xi_k,\tau)}{\partial \xi} = \sum_{j=1}^{n+2} A'_{kj} Y_{o,j}(\eta_i,\tau), \frac{\partial^2 Y_o(\eta_i,\xi_k,\tau)}{\partial \xi^2} = \sum_{j=1}^{n+2} B'_{kj} Y_{o,j}(\eta_i,\tau) \quad \text{(vii)}$$

Since the boundary conditions of Eq. (v-viii) of Appendix I are

$$X_i(\eta_1,\tau) = X_{i,1}(\tau) = 1, X_o(\eta_1,\tau) = X_{o,1}(\tau) = 1 \quad \text{(viii)}$$

$$\frac{\partial X_i(\eta_{n+2},\tau)}{\partial \eta} = 0, \quad \frac{\partial X_o(\eta_{n+2},\tau)}{\partial \eta} = 0 \quad \text{(ix)}$$

that is,

$$\sum_{j=1}^{n+2} A_{n+2,j} X_{i,j}(\tau) = 0, \sum_{j=1}^{n+2} A_{n+2,j} X_{o,j}(\tau) = 0 \quad \text{(ix-1)}$$

$$X_{i,n+2}(\tau) = -\left(A_{n+2,1} + \sum_{j=2}^{n+1} A_{n+2,j} X_{i,j}(\tau) \right) / A_{n+2,n+2} \quad \text{(x-1)}$$

$$X_{o,n+2}(\tau) = -\left(A_{n+2,1} + \sum_{j=2}^{n+1} A_{n+2,j} X_{o,j}(\tau) \right) / A_{n+2,n+2} \quad \text{(x-2)}$$

By following the same procedure for Y_i and Y_o,

$$Y_i(\eta_i, \xi_1, \tau) = Y_{i,1}(\eta_i, \tau) = X_i(\eta_i, \tau) \quad \text{(xi-1)}$$

$$Y_o(\eta_i, \xi_1, \tau) = Y_{o,1}(\eta_i, \tau) = X_o(\eta_i, \tau) \quad \text{(xi-2)}$$

$$Y_{i,n+2}(\eta_i,\tau) = -\left(A'_{n+2,1} X_i(\eta_i,\tau) + \beta_{11}(X_i(\eta_i,\tau) - Z_i(\eta_i,\tau)) + \sum_{j=2}^{n+1} A'_{n+2,j} Y_{i,j}(\eta_i,\tau) \right) / A'_{n+2,n+2} \quad \text{(xii-1)}$$

$$Y_{o,n+2}(\eta_i,\tau) = -\left(A'_{n+2,1} X_o(\eta_i,\tau) + \sum_{j=2}^{n+1} A'_{n+2,j} Y_{o,j}(\eta_i,\tau) \right) / A'_{n+2,n+2} \quad \text{(xii-2)}$$

Inserting Eq. (viii-xii) into Eq. (iv-vii),

$$\frac{\partial X_i(\eta_i,\tau)}{\partial \eta} = \left(A_{i1} - A_{i,n+2} \frac{A_{n+2,1}}{A_{n+2,n+2}} \right) + \sum_{j=2}^{n+1} \left(A_{ij} - A_{i,n+2} \frac{A_{n+2,j}}{A_{n+2,n+2}} \right) X_{i,j}(\tau)$$

$$\frac{\partial^2 X_i(\eta_i,\tau)}{\partial \eta^2} = \left(B_{i1} - B_{i,n+2} \frac{A_{n+2,1}}{A_{n+2,n+2}} \right) + \sum_{j=2}^{n+1} \left(B_{ij} - B_{i,n+2} \frac{A_{n+2,j}}{A_{n+2,n+2}} \right) X_{i,j}(\tau)$$

$$\frac{\partial X_o(\eta_i,\tau)}{\partial \eta} = \left(A_{i1} - A_{i,n+2} \frac{A_{n+2,1}}{A_{n+2,n+2}} \right) + \sum_{j=2}^{n+1} \left(A_{ij} - A_{i,n+2} \frac{A_{n+2,j}}{A_{n+2,n+2}} \right) X_{o,j}(t)$$

$$\frac{\partial^2 X_o(\eta_i,\tau)}{\partial \eta^2} = \left(B_{i1} - B_{i,n+2} \frac{A_{n+2,1}}{A_{n+2,n+2}} \right) + \sum_{j=2}^{n+1} \left(B_{ij} - B_{i,n+2} \frac{A_{n+2,j}}{A_{n+2,n+2}} \right) X_{o,j}(t)$$

$$\frac{\partial Y_i(\eta_i,\xi_1,\tau)}{\partial \xi} = \sum_{j=1}^{n+2} A'_{1j} Y_{i,j}(\eta_i,\tau)$$

$$= A'_{11} Y_{i,1}(\eta_i,\tau) + \sum_{j=2}^{n+1} A'_{1j} Y_{i,j}(\eta_i,\tau) + A'_{1,n+2} Y_{i,n+2}(\eta_i,\tau)$$

$$= A'_{11} X_{i,1}(\eta_i,\tau) + \sum_{j=2}^{n+1} A'_{1j} Y_{i,j}(\eta_i,\tau) - A'_{1,n+2} \left(A'_{n+2,1} X_i(\eta_i,\tau) + \beta_{11}(X_i(\eta_i,\tau) - Z_i(\eta_i,\tau)) + \sum_{j=2}^{n+1} A'_{n+2,j} Y_{i,j}(\eta_i,\tau) \right) / A'_{n+2,n+2}$$

$$\frac{\partial Y_i(\eta_i,\xi_1,\tau)}{\partial \xi} = \left(A'_{11} - A'_{1,n+2} \frac{A'_{n+2,1}}{A'_{n+2,n+2}} \right) X_i(\eta_i,\tau) - A'_{1,n+2} \frac{\beta_{11}}{A'_{n+2,n+2}} (X_i(\eta_i,\tau) - Z_i(\eta_i,\tau)) + \sum_{j=2}^{n+1} \left(A'_{1j} - A'_{1,n+2} \frac{A'_{n+2,j}}{A'_{n+2,n+2}} \right) Y_{i,j}(\eta_i,\tau)$$

$$\frac{\partial Y_o(\eta_i,\xi_1,\tau)}{\partial \xi} = \left(A'_{11} - A'_{1,n+2} \frac{A'_{n+2,1}}{A'_{n+2,n+2}} \right) X_o(\eta_i,\tau) + \sum_{j=2}^{n+1} \left(A'_{1j} - A'_{1,n+2} \frac{A'_{n+2,j}}{A'_{n+2,n+2}} \right) Y_{o,j}(\eta_i,\tau)$$

$$\frac{\partial^2 Y_i(\eta_i,\xi_k,\tau)}{\partial \xi^2} = \left(B'_{k1} - B'_{k,n+2} \frac{A'_{n+2,1}}{A'_{n+2,n+2}} \right) X_i(\eta_i,\tau) - B'_{k,n+2} \frac{\beta_{11}}{A'_{n+2,n+2}} (X_i(\eta_i,\tau) - Z_i(\eta_i,\tau)) + \sum_{j=2}^{n+1} \left(B'_{kj} - B'_{k,n+2} \frac{A'_{n+2,j}}{A'_{n+2,n+2}} \right) Y_{i,j}(\eta_i,\tau)$$

$$\frac{\partial^2 Y_o(\eta_i,\xi_k,\tau)}{\partial \xi^2} = \left(B'_{k1} - B'_{k,n+2} \frac{A'_{n+2,1}}{A'_{n+2,n+2}} \right) X_o(\eta_i,\tau) + \sum_{j=2}^{n+1} \left(B'_{kj} - B'_{k,n+2} \frac{A'_{n+2,j}}{A'_{n+2,n+2}} \right) Y_{o,j}(\eta_i,\tau)$$

After substituting the above partial differentials into Eq. (i, ii, ix, x) of Appendix I, one can solve the resulting ordinary differential equations using Gear's method.

NOMENCLATURE

- A_s^* : total surface area available for biolayer formation and adsorption per unit volume of biofilter [cm^{-1}]
- A_{si} : biolayer surface area per unit volume of reactor, for VOC i [cm^{-1}]
- c_i : concentration of substance i in the air at a position h along the biofilter [g cm^{-3}]
- $c_{i,o}$: value of c_i at t=0 [g cm^{-3}]
- c_o : oxygen concentration in the air at a position h along the biofilter [gm^{-3}]
- $c_{o,0}$: value of c_o at t=0 [gm^{-3}]
- C_i : inlet concentration of VOCs [gm^{-3}]
- C_o : outlet concentration of VOCs [gm^{-3}]
- C_{T0} : inlet concentration of toluene [gm^{-3}]
- D_i : diffusion coefficient of pollutant i in the biofilm [cm^2sec^{-1}]
- D_l : dispersion coefficient [cm^2sec^{-1}]
- D_o : diffusion coefficient of oxygen in the biofilm [cm^2sec^{-1}]
- e_i : effectiveness factor based on pollutant i
- e_o : effectiveness factor based on oxygen
- h : position in the column. m: h=0 at he entrance, h=L at the exit

$k_{i, g\text{-}ads}$: mass-transfer coefficient of component i between the gas and the solid particle [sec^{-1}]
$K_{I, i}$: inhibition constant in the specific growth rate expression of a culture growing on compound i [g cm^{-3}]
$k_{i, l\text{-}ads}$: mass-transfer coefficient of component i between the liquid and the solid particle [sec^{-1}]
$K_{m, i}$: constant in the reaction rate expression of a culture growing on compound i [g cm^{-3}]
$K_{O, i}$: constant in the specific growth rate expression of a culture expressing the effect of oxygen [g cm^{-3}]
$k_{rxn, i'}$: first-order reaction rate constant of component i in the adsorbent [sec^{-1}]
L : total height of the biofilter bed. m
$m_{1, i}$: distribution coefficient for the substance i in an air/water system
$m_{2, i}$: distribution coefficient for the substance i in an air/solid media system
m_O : distribution coefficient for the oxygen in an air/water system
n' : order of reaction in the adsorbent
q_i : concentration of component i on the solid particle [g cm^{-3}]
$q^*_{i, g\text{-}ads}$: equilibrium concentration of component i on the solid particle [g cm^{-3}]
$R_{i, ads}$: rate of generation of component i in the adsorbed phase [g cm^{-3} sec^{-1}]
$R_{i, film}$: rate of generation of component i in the biofilm [g cm^{-3} sec^{-1}]
$R_{max, i}$: reaction rate constant of component i [g cm^{-3} sec^{-1}]
$R_{max, o}$: reaction rate constant of oxygen [g cm^{-3} sec^{-1}]
$R_{o, film}$: rate of generation of oxygen in the biofilm [g cm^{-3} sec^{-1}]
s_i : concentration of pollutant i at a position x in the biolayer at a point h along the column [g cm^{-3}]
s_o : concentration of oxygen at a position x in the biolayer at a point h along the column [g cm^{-3}]
t : time [sec]
υ : interstitial gas velocity in the biofilter [cm sec^{-1}]
V_p : volume of the biofilter bed [cm^3]
x : position in the biolayer [cm]
X_v : biofilm density [g cm^{-3}]
Y_i : yield coefficient of a culture on VOC i [g g^{-1}]
Y_{oi} : yield coefficient of a culture on oxygen [g g^{-1}]
z : position from the inlet of the bed

Greek Letters

α : fraction of total surface area available for biofilm formation
δ : effective biolayer thickness [cm]
ε : porosity of the biofilter bed
μ_i^* : specific growth rate [sec^{-1}]
ρ_p : density of the solid particles [g cm^{-3}]

REFERENCES

Abumaizar, R. J., Smith, E. H. and Kocher, W., "Analytical Model of Dual-media Biofilter for Removal of Organic Air Pollutants," *J. Environ. Eng. Div. (Am. Soc. Civ. Eng.)*, **123**(6), 606 (1997).

Amanullah, Md., Farooq, S. and Viswanathan, S., "Modeling and Simulation of a Biofilter," *Ind. Eng. Chem. Res*., **38**, 2765 (1999).

Baider, F. G., "Kinetics of Double-substrate-limited Growth," In Microbial Population Dynamics, Bazin, M. J., CRC Press, Boca Raton, FL (1982).

Chaudhary, D. S., Vigneswaran, S. and Ngo, H. H., "Biofilter in Water and Wastewater Treatment," *Korean J. Chem. Eng.*, **20**, 1054 (2003).

Deshusses, M. A., Hamer, G. and Dunn, I. J., "Behavior of Biofilters for Waste Air Biotreatment. 1. Dynamic Model Development," *Environ. Sci. Technol*., **29**(4), 1048 (1995).

Devinny, J. S., Deshusses, M. A. and Webster, T. S., "Biofiltration for air Pollution Control," Lewis publishers, Washington D.C. (1999).

Diks, R. M. M. and Ottengraf, S. P. P., "Verification Studies of a Simplified Model for Removal of Dichloromethane from Waste Gases using a Biological Trickling Filter," *Bioprocess Engng*., **6**, 93 (1991).

Fan, L. S., Leyva-Ramos, R., Wisecarver, K. D. and Zehner, B. J., "Diffusion of Phenol through a Biofilm grown on Activated Carbon Particles in a Draft-tube Three-phase Fluidized-bed Bioreactor," *Biotechnol. Bioeng.*, **35**, 279 (1990).

Hodge, D. S. and Devinny, J. S., "Modeling Removal of Air Contaminants by Biofiltration," *J. Environ. Eng. Div. (Am. Soc. Civ. Eng.)*, **121**(1), 21 (1995).

Jennings, P. A., Snoeyink, V. L. and Chian, E. S. K., "Theoretical Model for a Submerged Biological Filter," *Biotechnol. Bioeng*., **18**, 1249 (1976).

Lim, K. H. and Lee, E. J., "Biofilter Modeling for Waste Air Treatment: Comparisons of Inherent Characteristics of Biofilter Models," *Korean J. Chem. Eng.*, **20**, 315 (2003).

Oh, K. J., Kim, Y. S. and Cho, S. K., "Degradation of Benzene and Toluene by a Fluidized Bed Bioreactor Including Microbial Consortium," *Korean J. Chem. Eng.*, **19**, 1026 (2002).

Ottengraf, S. P. P., "Theoretical Model for a Submerged Biological Filter," *Biotechnol. Bioengng*., **19**, 1411 (1977).

Shareefdeen, Z., Baltzis, B. C., Oh, Y. S. and Bartha, R., "Biofiltration of Methanol Vapor," *Biotechnol. Bioengng*, **41**, 512 (1993).

Shareefdeen, Z. and Baltzis, B. C., "Biological Removal of Hydrophobic Solvent Vapors from Airstreams," In Advances in bioprocess engineering, Galindo, E., Ramirez, O. T., Eds., Kluwer Academic Publishers, Dordrecht, The Netherlands (1994).

Shareefdeen, Z. and Baltzis, B. C., "Biofiltration of Toluene Vapor under Steady-state and Transient Conditions: Theory and Experimental Results," *Chem. Eng. Sci.*, **49**, 4347 (1994).

Yoon, I.-K., Kim, C.-N. and Park, C.-H., "Optimum Operating Conditions for the Removal of Volatile Organic Compounds in a Compost-Packed Biofilter," *Korean J. Chem. Eng.*, **19**, 954 (2002).

Zarook, S. M. and Shaikh, A. A., "Analysis and Comparison of Biofilter Models," *Chem. Eng. J.*, **65**, 55 (1997).